Maschotta, Ralph; Rehs, Jörg; Boymann, Simon; Hoppe, Ulrich :

Evaluation of feature extraction algrorithms for the feature-list cross-correlation in retinal images

Zuerst erschienen in:
EMBEC '05 : 3rd European Medical & Biological Engineering Conference, November 20 - 25, 2005, Prague, Czech Republic / International Federation for Medical and Biological Engineering
Prague, 2005
IFMBE proceedings ; 11

EVALUATION OF FEATURE EXTRACTION ALGORITHMS FOR THE FEATURE-LIST CROSS-CORRELATION IN RETINAL IMAGES

R. Maschotta*, J. Rehs*, S. Boymann* and U. Hoppe**

* Institute of Biomedical Engineering and Informatics, Technical University Ilmenau, Ilmenau, Germany
** Department of Audiology, University Hospital of Erlangen-Nuremberg, Erlangen, Germany

Ralph.Maschotta@TU-Ilmenau.de

Abstract: In this paper the results of different feature extraction algorithms are used to build feature-lists. These feature-lists are used for motion estimation in retinal fundus image series. Therefore the feature-list cross-correlation algorithm is used. The influence of the feature extraction on the results of the feature-list cross-correlation is evaluated. Therefore different kind of image series, with different kind of selected templates is used. The reference position is determined by the median of the detected position of all templates and all feature extraction algorithms. The amount of incorrect detected templates is compared.
The Harris corner detector detects only the optic nerve sufficiently. The Sobel-operator delivers the best results, except using small templates. The Canny-edge-detection has good results too. Over all, the rule-based edge detection delivers the best result.
Generally, it is possible to use different feature extraction algorithms to estimate motions in retinal image series by using feature-list cross-correlation algorithms.
As long as the amount of feature values of the template or the image is much smaller than the amount of pixels in the image, the feature-list cross-correlation algorithms are faster than the common cross-correlation algorithms.

Introduction

Cross-correlation algorithms are widely used in image processing for motion analysis [1]. Unfortunately, these algorithms are usually sensitive to changes in brightness, contrast and noise. Furthermore, rotation, scaling or other image distortions cause high processing effort. Therefore, a number of algorithms with reduced computational effort were developed. For instance, frequency based matching, wavelet matching, feature- or texture-based techniques are used. In this paper feature-list cross-correlation algorithms are analyzed [2],[3]. Obviously, the results of the feature-list cross-correlation algorithm depend on the selected feature extraction algorithm. Therefore, the selected feature extraction should be robust and with a minimum of values unequal zero.

The aim of this paper is to investigate the application of different feature extraction algorithms like edge detection [4],[5] and corner detection algorithms [6] to retinal image series. Human retinal images have a high intraindividual reproducibility and do usually not change even in longer time intervals.

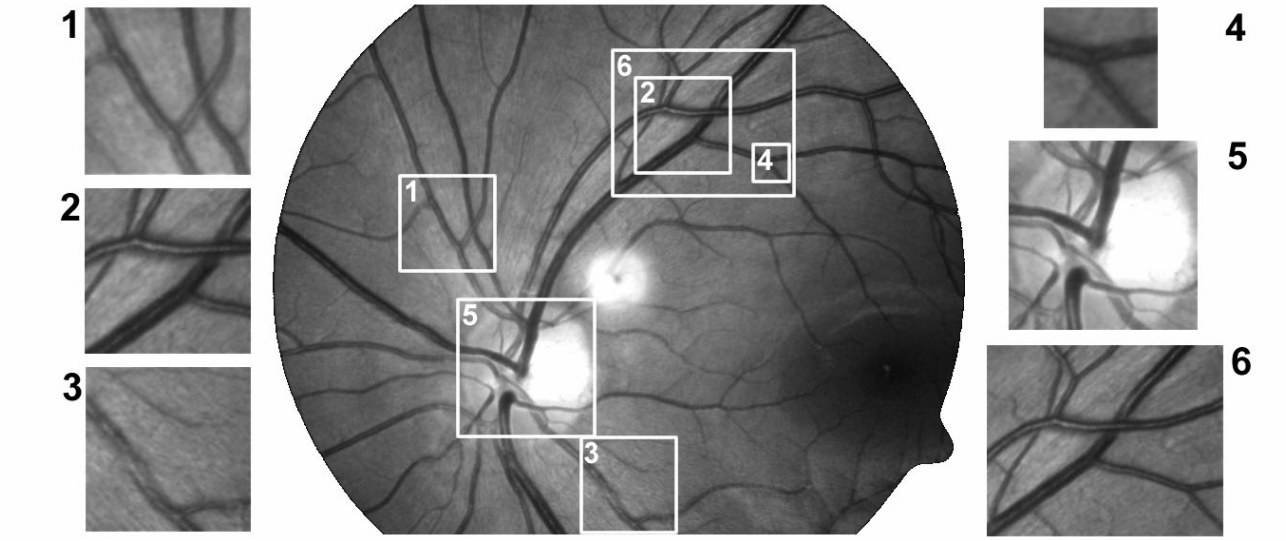

Figure 1: Example of retinal fundus image with the selected template. 1-3: medium template (100x100 pixel); 4: small template (40x40 pixel); 5: template wich include the optic nerve (180x180 pixel); 6: Large template (240x140 pixel)

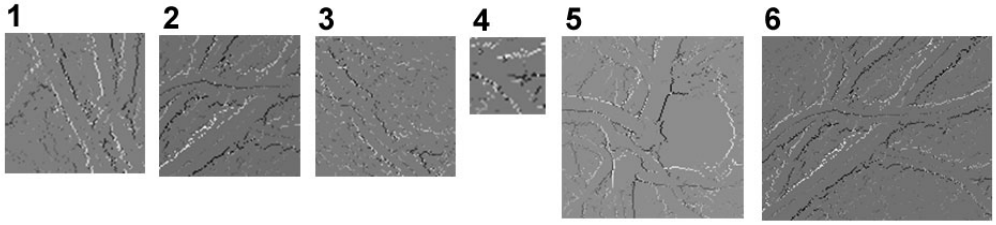

Figure 2: Example of the result of the rule-based edge detection for the templates (see Figure 1). White: value of negative gradient, Black: value of positive gradient

Materials and Methods

For this analysis two different types of retinal image series were used. The first type of image series has been recorded by the Retinal Vessel Analyzer (RVA) with a Zeiss FF-450 fundus camera [7]. They consist of two image series of 182 and 251 images of two healthy subjects. The images have a size of 760x570 pixels.

The second type of image series has been recorded by the VisualIS system for digital fundus imaging (Imedos GmbH, Jena). This image series includes 22 to 24 single grayscale fundus images of five healthy subjects. The images have a size of 768x576 pixels. These images have a better quality, because short flashes were used as fundus illumination. Additional an optical green filter of 560nm is used. In total, 433 images of lower quality (first type of image series) and 114 with good quality were analyzed.

The first type of image series is disturbed by noise. In order to reduce noise, the images of the first type of image series are smoothed by Gaussian filter with a size of 5x5 pixels.

The second type of image series is disturbed by light reflections caused by a experimental environment. This reflection produces a bright spot (see Figure 1). This spot is always at the same position. Hence, these specular reflections are eliminated by omitting the corresponding region.

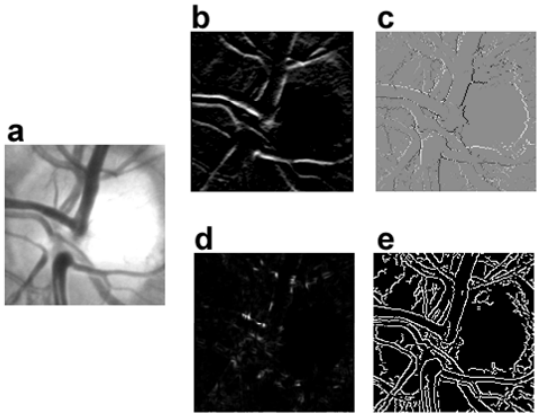

Figure 3: Result of the different feature extraction algorithms. a: original image of template 5 (see Figure 1); b: Sobel-Operator; c: rule-based edge detection; d: Harris-corner-detection e: Canny-edge-detection

Six templates of different size showing different image details for each image series are analyzed. The templates are manually selected for each image series. Three of these templates include characteristic vessels. They have a size of 100x100 pixels. One small template is used. This template includes a single junction of a fine vessel. It has a size of approximately 40x40 pixels. Furthermore, one large template with a size of approximately 180x180 pixels is used. This template includes the optic nerve. Finally another large template with approximately 240x140 pixels is used. This template includes multiple junctions of vessels.

The results of the feature extraction are saved in feature lists. The feature-list includes the x and y position and the value of the feature b[b,y]:

$$\begin{aligned} b_x[n] &= x \\ b_y[n] &= y \\ b_v[n] &= b[x,y] \end{aligned} \qquad (1)$$

where
x=1…N_b, (Number of rows)
y=1…M_b, (Number of columns)
n=1…S, (Number of list entrys)

Where M_b x N_b is the size of the image. The basis of the feature-list cross-correlation algorithm is the two dimensional cross-correlation algorithm:

$$g[x,y] = \sum_{i,j} \mathrm{h[x,\,y]b[x+i,\,y+j]} \qquad (2)$$

where
x=1, … ,N_b,
y=1, … ,M_b,
i=-$\frac{(N_h-1)}{2}$, … ,$\frac{(N_h-1)}{2}$
j=-$\frac{(M_h-1)}{2}$, … ,$\frac{(M_h-1)}{2}$

Where M_b,N_b is the size of the image and M_h,N_h is the size of the template. The feature-list cross-correlation algorithm is defined as follows:

$$g[x,y] = \sum_{i=1}^{S_b}\sum_{j=1}^{S_h} c_{i,j} \cdot P_{x,y,i,j} \qquad (3)$$

where
$c_{i,j} = b_v[i] \cdot h_v[i]$
$P_{x,y,i,j} = \delta\left(x-\left(b_x[i]-h_x[j]\right)\right)\cdot\delta\left(y-\left(b_y[i]-h_y[j]\right)\right)$

where $\delta(x) = \begin{cases} 1 & for \quad x=0 \\ 0 & for \quad x\neq 0 \end{cases}$

for $x=1\ldots N_g, \quad y=1\ldots M_g$

The position where P≠0 can be calculated by:

$$x = (b_x[i] - h_x[j])$$
$$y = (b_y[i] - h_y[j]) \quad (4)$$

By examining formula (3) it can be concluded, that the result is influenced by the product, only if both values $b_v[i]$ and $h_v[j]$ are not equal zero (5). Therefore only feature values, which are not equal zero, are saved in the feature list. As a result the processing time decreases. Former studies on analytic images have shown that the feature-list cross-correlation algorithm based on difference (6) delivers the best results [2],[3]. Therefore, this method is used as follows.

$$c_{i,j} = \begin{cases} 0 & for \quad b_v[i] = 0 \quad \vee \quad h_v[j] = 0 \\ b_v[i] \cdot h_v[j] & else \end{cases} \quad (5)$$

$$c_{i,j} = \begin{cases} 0 & for \quad b_v[i] = 0 \quad \vee \quad h_v[j] = 0 \\ 255 - (b_v[i] - h_v[j]) & else \end{cases} \quad (6)$$

The difference doesn't fulfill the condition (5). Therefore condition (5) is adapted to match the difference algorithm.

Different edge and corner detection algorithms are used to calculate simple features. After computing the image or the template every value above a threshold value is used as one feature value. The same threshold values or parameter values are used for all images and templates.

The first edge detection algorithm uses the common 3x3 Sobel-operator. The signed results in horizontal and vertical direction are saved in one feature list. The second feature extraction algorithm is the common Canny-edge-detection. The next feature extraction algorithm is a rule-based edge detection algorithm [5]. The rule-based edge detection algorithm uses two different one-dimensional operators with different size (7). The operators are convolved with the image.

$$F0 = [1, -1]$$
$$F1 = [1,4,6,4,-15] \quad (7)$$

The results are combined with a deterministic finite automat (see Figure 4). Only those signed results are added to the feature list, whose absolute value is greater than a threshold value. The results of both directions are listed into one feature list.

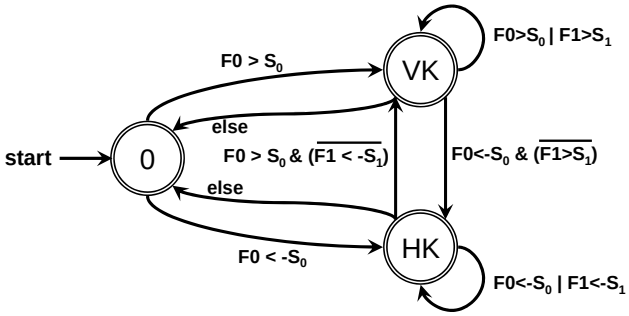

Figure 4: Deterministic finite automat of the rule-based edge detection. S: treshold values, HK/VK: edge states

The last feature is computed by the Harris-corner-detector [6]. All result values greater than a threshold value are added to the feature list, not only the local maximum values.

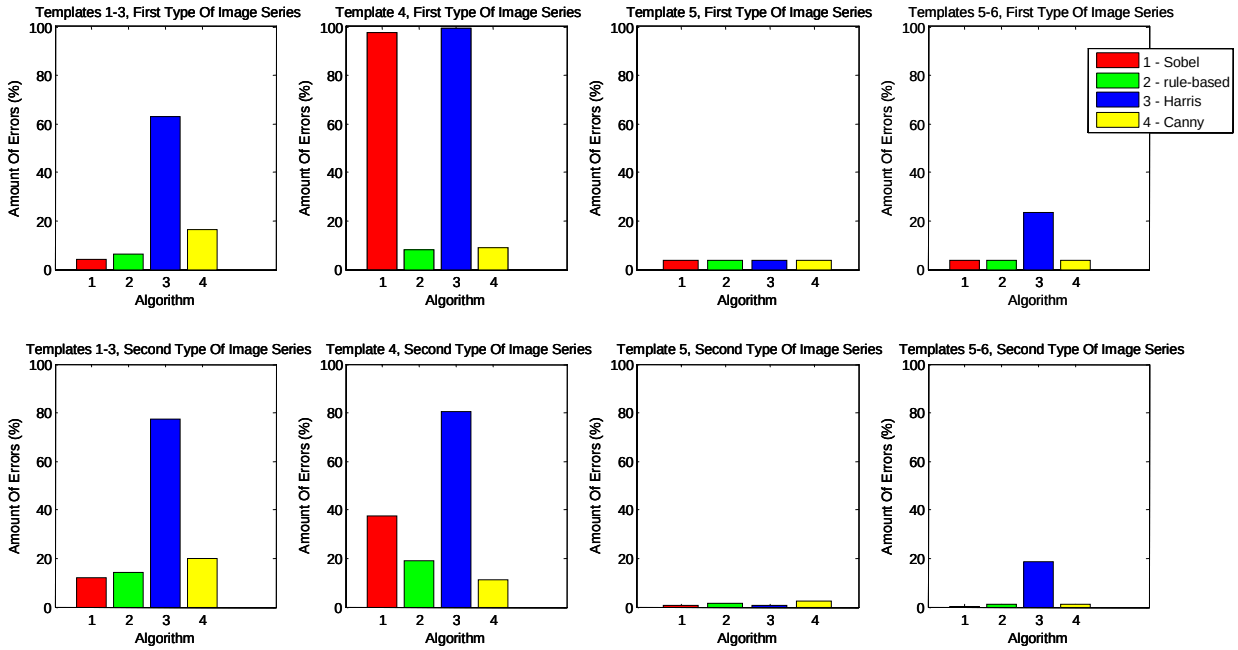

Figure 5: Amount of incorrect detected templates in percent. Top: first type of image series (433 images); Bottom: second type of image series (114 images); Result of the: 1 - Sobel-operator, 2 - rule-based edge detection, 3 - Harris-corner-detection, 4 - Canny-edge-detection; Template 1-3: medium templates with a size of 100x100 pixels; Template 4: small template (40x40 pixels); Template 5: image which includes the optic nerve; Template 5-6: Large templates

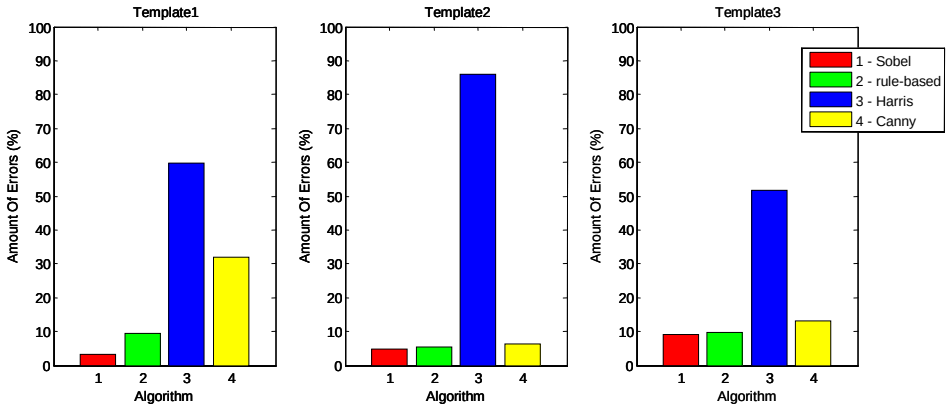

Figure 6: Amount of incorrect detected templates in percent with regard to the contents of the image. The size of the template is constant.

The displacements of the images are unknown. But for each image 4 different matching algorithms use 6 different templates to calculate 24 different positions. The x and y displacements of the first image are calculated. The median values of the 24 x and y displacements are used as reference for the probably correct displacement. If the distance from the calculated reference in x or y direction is greater than five pixels, the result is defined as incorrect. The amount of all incorrect detected templates is compared. Therefore the results of the different feature extraction algorithms are analyzed with regard to the size of the template, the content of the image and the kind of image sequence.

Results

At the top of Figure 5 the results of the first type of image series are shown. At the bottom the results of the second type of image series are shown. In the first column the results of the templates with the size of 100x100 are shown. The results of the small templates are following. The results of the templates including the optic nerve are displayed in the third column. The last column shows the results of the large templates.

The difference between the first and the second image series are minimal. Only the results of template 4 show little variations.

The differences between the several types of templates are considerable. The Sobel-operator delivers the best results for the first group of templates, which have a size of 100x100 pixels. The next best algorithms are the rule-based edge detection and the Canny-edge-detection.

The small template causes the highest amount of incorrect detected templates. The Harris corner detector doesn't find the small template in the first image series. In the second type of image series the small template is detected seldomly with this feature extraction algorithm. The Sobel-operator rarely detects the small template. The Canny-edge-detection produces the best results with this type of templates in the second type of image series. In the first type of image series the rule-based edge detection delivers the best results.

The templates which include the optic nerve (template 5) are detected very well by all feature detection algorithms. Also the large templates (templates 5 and 6) are detected very well. Only the Harris-corner-detection has a significant amount of incorrect detected templates.

Figure 6 shows the result of the cross-correlation with regard to the contents of the image. The templates 1-3 have the same size. The results of the Harris- and the Canny-edge-detection are varying. The results of the other feature extraction are almost constant. In Figure 7 the amount of all incorrect detected templates for all image series are shown. The rule-based edge detection produces the best results, followed by the Canny-edge-detection and the Sobel-operator. The Harris-corner-detection produces the highest amount of incorrect detected templates. Only the template including the optic nerve (see Figure 5) is detected by the Harris corner detector.

By using feature list cross-correlation algorithms, the time effort depends on the length of the feature list. Hence, the Canny and the rule-based edge detection algorithm are faster than the Sobel-operator. The Harris-corner-detector needs the highest processing effort.

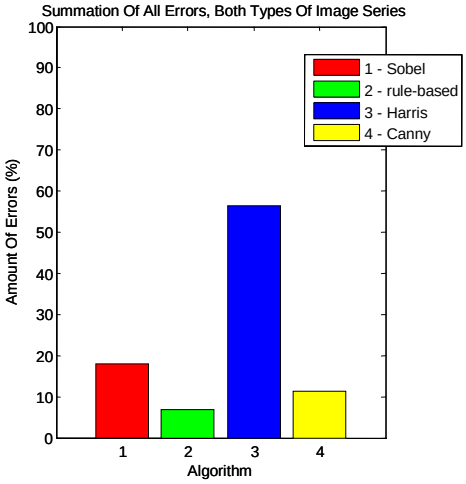

Figure 7: Amount of incorrect detected templates for all images in percent.

Discussion

Large templates are detected very well. If the template size decreases, the amount of incorrect detected templates is rising. But the size is not the major magnitude of influence. The selected templates include a different amount of unique vessel structures.

Large templates include more unique structures. Therefore it is possible to detect these templates easily. If the size decreases, the amount of unique structures in the image decreases too. Hence, the amount of incorrect detected templates is rising.

The type of feature extraction has also a major influence on the result of the cross correlation.

The Harris corner detector only detects the optic nerve sufficiently. The reason might be, that only in this area the feature-values are very high. Additionally the pure result values of the Harris-corner detector are used without local maximum detection. Moreover, the same settings for all analyses are used. But the feature values differ very strong within the same image. Therefore the selection of a threshold value which is useful for all templates and image series is crucial. The additional automatic selection of unique local maxima can improve the results. Additionally, the amount of feature values is strongly decreased. Therefore, the computation effort could be strongly decreased as well.

Without the result of the small templates the Sobel-operator delivers the best results. If the template is too small the cross-correlation results are poor. Hence, it can be assumed that the cross-correlation algorithm can't differentiate similar structures by using the Sobel-operator. In reverse it can be assumed that the cross-correlation algorithm can detect similar structures. This will be subject of future analysis.

The Canny-edge-detection is a common feature extraction algorithm with good results. But the results are more depending on the content of the image compared to the results of other feature extraction algorithms. If the template is well chosen, the cross-correlation algorithm produces good results.

Altogether, the rule-based feature extraction delivers the best results. The amount of detected features is also small. Therefore, the computation effort is very low.

In this analysis all algorithms have to use the same settings for all images. To enhance the result it is possible to adjust the settings for each kind of image series. Adaptive algorithms could be used to prevent manual settings. Moreover, the settings can be adapted to dynamic change of image conditions.

The selection of the template has an influence on the result. More different templates and more different image series have to be used to analyze this influence. Moreover, templates which are not in the images have to be used, to evaluate the influence of the feature extraction on the sensitivity and specifity. Furthermore, the first image series was smoothed by Gaussian filter. The influence of smoothing could be analyzed by using more different filters. Finally, the influence of the feature extraction algorithms on the amount of the coefficients and the Peak Signal to Noise Ratio (PSNR) has to be analyzed.

Conclusions

Common feature extraction algorithms can be used for motion estimation by using feature-list cross-correlation algorithms. The results of the cross-correlation algorithms are depending on the type of the feature extraction, the size and the content of the used template. For noisy images smoothing is an important preprocessing for proper results. For large templates the Sobel-operator gives the best results. By using small templates the Canny-edge-detection delivers the best results. Regarding all images and templates, best results were retrieved when the rule-based edge detection was used.

As long as the amount of feature values of the template or the image is much smaller than the amount of pixels in the image, the feature-list cross-correlation algorithms are much faster than common cross correlation algorithms.

Acknowledgement

We thank Dr. E. Nagel (ophthalmologic practice Rudolstadt) and Imedos GmbH Jena for providing the image series.

References

[1] C. Stiller, J. Konrad: Estimating motion in image sequences: A tutorial on modeling and computation of 2d motion, in IEEE Signal Processing Magazine, July 1999, pp. 70-91.

[2] R. Maschotta, S. Boymann, D. Steuer: Shift reducing of retinal vessel image series by using edge based template matching algorithm, in Proc. of 2nd EMBEC, Wien, 2002, pp. 848-849.

[3] R. Maschotta, M. Pietraszczyk, S. Boymann, D. Jannek: Genauigkeit und Generalisierbarkeit kantenlistenbasierter Korrelationsverfahren im Vergleich zu grauwertbasierten Verfahren, in Proc. of Bildverarbeitung für die Medizin (BVM), Berlin, 2004, pp. 110-114.

[4] J. Canny: A computational approach to edge detection, in IEEE Transactions on Pattern Analysis and Machine Intelligence, volume 8, 1986, pp. 679-698.

[5] R. Maschotta, S. Boymann, U. Hoppe: Regelbasierte Kantenerkennung zur schnellen kantenbasierten Segmentierung der Glottis in Hochgeschwindig-keitsvideos, in Proc. of Bildverarbeitung für die Medizin (BVM), Heidelberg, 2005, pp. 188-192.

[6] C. Harris, M. Stephens: A Combined Corner and Edge Detector, in Proc. of 4th Alvey Conference, 1988, pp. 147-151.

[7] W. Vilser, T. Riemer, E. Nagel, A. Fink et. al.: Functional imaging of retinal vessels - principle and clinical potential, in Proc of. 38th Annual Congress of the German Society for Biomedical Engineering (BMT), Ilmenau, 2004, pp. 804-805.